Stability of Quark Star Models

2016 Commun. Theor. Phys. 65 575

(http://iopscience.iop.org/0253-6102/65/5/575)

Commun. Theor. Phys. **65** (2016) 575–584 Vol. 65, No. 5, May 1, 2016

Stability of Quark Star Models

M. Azam,[1,*] S.A. Mardan,[2,†] and M.A. Rehman[2,‡]

[1]Division of Science and Technology, University of Education, Township Campus, Lahore-54590, Pakistan

[2]Department of Mathematics, University of the Management and Technology, C-II, Johar Town, Lahore-54590, Pakistan

(Received January 4, 2016; revised manuscript received March 1, 2016)

Abstract *In this paper, we investigate the stability of quark stars with four different types of inner matter configurations; isotropic, charged isotropic, anisotropic and charged anisotropic by using the concept of cracking. For this purpose, we have applied local density perturbations technique to the hydrostatic equilibrium equation as well as on physical parameters involved in the model. We conclude that quark stars become potentially unstable when inner matter configuration is changed and electromagnetic field is applied.*

PACS numbers: 04.20.-q, 04.40.Dg, 04.50.Gh
Key words: quark stars, cracking, density perturbations, electromagnetic field

1 Introduction

Strange matter (bulk quark matter) has been hypothesized to be more stable than hadronic matter.[1] Thus a natural question arises about the existence of strange stars (SS) which are composed of strange matter. It is very difficult to discriminate between neutron stars (NS) and SS, since both share many similarities in observational phenomenon. But these objects can be discriminated on the basis of mass-radius relation. In this context, Li *et al.*[2] argued that Her X-1 star is a good candidate for SS. The possible existence of SS is a direct result of hypothesis that strange matter is the ground state of strongly interacting matter. Bombaci[3] provides observational evidence for possible existence of strange matter in x-ray buster 4U 1820-30. He found that the models of NS with conventional equation of state (EoS) cannot guarantee to have SS mass-radius relation for 4U 1820-30. However, for suitable choice of parameters SS models are consistent with 4U 1820-30. The arguments about x-ray pulsar Her X-1 and x-ray buster 4U 1820-30 to be SS were reinforced by Day *et al.*[4] They derived EoS for strange matter to calculate the mass-radius relation for SS which was in complete agrement with compact objects Her X-1 and 4U 1820-30.

Many authors presented quark stars (QS) models for charged and neutral strange matter. Mak and Harko[5] studied spherically symmetric charged QS model with one-parameter group of conformal motion and found a unique static charged configuration of quark strange matter with radius 9.46 km and total mass $2.86M_{\odot}$. Thirukkanesh and Maharaj[6] found a family of solutions for charged anisotropic matter and showed that they correspond with already discovered SS for suitable values of parameters. Negreiros *et al.*[7] described how electric field may effect mass and radii of QS. Gangopadhyay *et al.*[8] predicted new refined masses and radii of SS like 4U 1820-30 and Her X-1. QS occurs when matter is squeezed tightly together just before collapse of a star into a black hole. Matter in this state has some very unusual properties. For example, its pressure is largely independent of temperature and due to tightly squeezed atoms only the strong force has any significant influence on its behavior.

The models of QS are physically acceptable if they are stable towards perturbations. Therefore, it is interesting to study stability of QS models. In this scenario, Herrera[9] introduced the concept of cracking to study collapse of stellar objects. Cracking describes the behavior of inner matter distribution just after equilibrium state is perturbed. The cracking takes place in self-gravitating objects due to reversal of sign in radial forces.[10] Herrera[11] discussed the transverse cracking of self-gravitating objects by investigating the effects of axially symmetric perturbations on matter variables. Di Prisco[12] and coworkers proved that cracking would take place in spherical objects due to small fluctuations in local anisotropy. Hernandez[13−14] analyzed cracking with local and non-local EoS for spherically symmetric objects. Abreu[15] presented the idea of cracking through radial sound speed and tangential sound speed by considering the radial pressure P_r and tangential pressure P_t as a function of constant density ρ i.e. $P_r = P_r(\rho)$ and $P_t = P_t(\rho)$. Manjarrez *et al.*[16] extended the concept of cracking for charged fluid distributions. Gonzalez[17−18] presented the idea of local

*E-mail: azam.math@ue.edu.pk
†E-mail: syedalimardanazmi@yahoo.com; ali.azmi@umt.edu.pk
‡E-mail: aziz3037@yahoo.com; aziz.rehman@umt.edu.pk

density perturbations (DP) to discuss the idea of cracking for relativistic spheres. Azam *et al.*[19−20] applied the local DP scheme to find stability regions of compact objects.

The effect of charge on the physical properties like mass, expansion and gravitational collapse of stellar objects is widely discussed in general relativity (GR) and astrophysics. Bonnor[21−22] studied the impact of charge on spherical stellar objects and found that electric repulsions can halt the gravitational collapse. Ray *et al.*[23] found that the maximum limit of charge is approximately 10^{20} coulomb for a stable compact star. Sharif and Azam[24−25] analyzed the stability of spherical and cylindrical systems in the presence of electromagnetic field. In this work, we apply the idea of cracking to QS models with neutral and charged inner matter configurations. Here, we have taken local DP instead of global DP. The model presented by Maharaj *et al.*[26] is considered in this work, which can be used to discuss different QS models (isotropic, anisotropic, neutral and charged) for suitable values of parameters. The detailed physical analysis of this model for $A_0 = 0$ was given by Sunzu *et al.*[27] This choice of parameter was necessary to ensure that entropy vanishes at the stellar center.

This paper is arranged as follows. Section 2 deals with Einsten–Maxwell field and basic equations corresponding to charged anisotropic fluid. We have presented the general formalism to determine the cracking of isotropic, anisotropic, neutral and charged QS with local DP in Sec. 3. Section 4 investigates the stable and unstable regions of QS models. In the last Sec. 5, we conclude our results.

2 Einstein-Maxwell Field and Basic Equations

We consider the line element for a static spherically symmetric space time in curvature coordinates given by

$$\mathrm{d}s^2 = -\,\mathrm{e}^{2\nu}\mathrm{d}t^2 + \mathrm{e}^{2\lambda}\mathrm{d}r^2 + r^2(\mathrm{d}\theta^2 + \sin^2\theta\mathrm{d}\phi^2)\,, \quad (1)$$

where $0 \le \theta \le \pi$, $0 \le \phi < 2\pi$ and $\nu = \nu(r)$, $\lambda = \lambda(r)$ represent gravitational potentials and the Maxwell's equations are

$$F_{ab;c} + F_{bc;a} + F_{ca;b} = 0\,, \quad (2)$$

$$F^{ab}_{;b} = 4\pi J^a, \quad (3)$$

where F^{ab} is the electromagnetic field tensor, J is the four current density. The skew-symmetric electromagnetic field tensor can be decomposed as

$$F^{ab} = \begin{bmatrix} 0 & E_x & E_y & E_z \\ -E_x & 0 & B_z & B_y \\ -E_y & -B_z & 0 & B_x \\ -E_z & -B_y & -B_x & 0 \end{bmatrix}, \quad (4)$$

here, $\boldsymbol{E} = (E_x, E_y, E_z)$ is the electric field and $\boldsymbol{B} = (B_x, B_y, B_z)$ is the magnetic field. The energy-momentum tensor of electromagnetic field is given by

$$E_{ab} = F_{ac}F^c_b - \frac{1}{4}g_{ab}F_{cd}F^{cd}, \quad (5)$$

with electromagnetic field tensor F_{ab} and four current density J^a are defined by

$$F_{ab} = A_{b,a} - A_{a,b}, \quad J^a = \sigma u^a, \quad (6)$$

where A is the four potential and σ is the proper charge density while $u^a = \mathrm{e}^{-\nu}\delta^a_0$ is four vector velocity of the fluid. The four potential is defined as

$$A_a = (\phi(r), 0, 0, 0)\,. \quad (7)$$

Using this in above equation, we obtain the only non-zero component of skew-symmetric field tensor

$$F_{01} = -\phi'(r)\,, \quad (8)$$

which can also be written as

$$F^{01} = \mathrm{e}^{-2(\nu+\lambda)}\phi'(r) = \mathrm{e}^{-(\nu+\lambda)}E(r)\,, \quad (9)$$

where, we have used $E(r) = \mathrm{e}^{-(\nu+\lambda)}\phi'(r)$. The total energy-momentum tensor corresponding to charged anisotropic fluid sphere is defined as

$$T_{ab} = \mathrm{diag}\Big(-\rho - \frac{E^2}{2}, P_r - \frac{E^2}{2}, P_t + \frac{E^2}{2}, P_t + \frac{E^2}{2}\Big)\,. \quad (10)$$

The terms E, ρ, P_r and P_t correspond to electromagnetic field, energy density, radial pressure, and tangential pressure of the fluid respectively.

The synergy of energy-momentum tensor of electromagnetic field and matter are governed by system of field equations. These synergies of spherically symmetric metric corresponding to Einstein–Maxwell field equations are given by

$$G_{ab} = \kappa T_{ab} = \kappa(M_{ab} + E_{ab})\,, \quad (11)$$

where M_{ab} is the energy momentum tensor of the fluid inside the star. We have set the value of coupling constant $\kappa = 8\pi$ $(G = c = 1)$ in the geometric unit system. The non-zero components of Einstein–Maxwell field equations corresponding to Eqs. (1) and (10) are given by

$$1 + \mathrm{e}^{-2\lambda}(2r\lambda' - 1) = 8\pi r^2\rho + r^2\frac{E^2}{2}\,, \quad (12)$$

$$1 - \mathrm{e}^{-2\lambda}(2r\nu' + 1) = -8\pi r^2 P_r + r^2\frac{E^2}{2}\,, \quad (13)$$

$$\mathrm{e}^{-2\lambda}(\lambda' r - \nu' r - \nu'' r^2 + \nu'\lambda' r^2 - (\nu')^2 r^2) = -8\pi r^2 P_t - r^2\frac{E^2}{2}\,, \quad (14)$$

$$r^2\sigma = \mathrm{e}^{-\lambda}(r^2 E)'\,, \quad (15)$$

where "$'$" denotes the differentiation with respect to r. It is argued that the choice of EoS for fluid inside of the star plays a key role for its physical significance.[4] The EoS describes how physical quantities like radial pressure, tangential pressure and density are related to each other. In this work, we have used the linear EoS for strange matter to explore the stability of QS. The linear form is given

by

$$P_r = \frac{\rho - 4B}{3}\,, \tag{16}$$

where B is a constant related to the surface density of QS. If Massachusetts Institute of Technology (MIT) bag model for QS is considered then B is identified with the bag constant.[28]

Solving Eqs. (12)–(14) simultaneously, we obtain hydrostatic equilibrium equation (TOV) for anisotropic charged fluid

$$\frac{\mathrm{d}P_r}{\mathrm{d}r} = \frac{2(P_t - P_r)}{r} - (\rho + P_r)\nu' + \frac{E}{8\pi r^2}(r^2E)', \tag{17}$$

which shows that gradient of pressure is effected by charge and anisotropy of fluid. Using the relation $\mathrm{e}^{-2\lambda(r)} = 1 - 2M/r + Q^2/r^2$ in Eq. (17) gives

$$\begin{aligned}\Omega = &-\frac{\mathrm{d}P_r}{\mathrm{d}r} + \frac{2(P_t - P_r)}{r} \\ &+ (\rho + P_r)\frac{-4M/r + 3r^2E^2 - 8\pi r^2 P_r}{4r(1 - 2M/r + r^2E^2)} \\ &+ \frac{(r^2E)'E}{8\pi r^2} = 0\,.\end{aligned} \tag{18}$$

Equation (18) describes the behavior of charged anisotropic inner fluid of compact star just after equilibrium state is perturbed. We will use Eq. (18) to discuss the cracking of QS for different inner matter configurations as it can be reduced to uncharge case by taking $E = 0$ and isotropic case by assuming $P_t - P_r = 0$.

3 Effect of Local Density Perturbation

We apply local DP,[17−18] i.e. $\delta\rho$ on charged QS in equilibrium state. From Eq. (18), it is clear that cracking takes place in interior fluid of QS when equilibrium state is interrupted due to change in sign of perturbed force and vice-versa. We apply the local DP to perturb all the physical variables like mass, radial and tangential pressure, electromagnetic field and their derivatives involve in Eq. (18), given by

$$P_r(\rho + \delta\rho) = P_r(\rho) + \frac{\mathrm{d}P_r}{\mathrm{d}\rho}\delta\rho\,, \tag{19}$$

$$\begin{aligned}\frac{\mathrm{d}P_r}{\mathrm{d}r}(\rho + \delta\rho) = &\frac{\mathrm{d}P_r}{\mathrm{d}r}(\rho) + \Big[\frac{\mathrm{d}}{\mathrm{d}r}\Big(\frac{\mathrm{d}P_r}{\mathrm{d}\rho}\Big) \\ &+ \frac{\mathrm{d}P_r}{\mathrm{d}\rho}\frac{\mathrm{d}^2\rho}{\mathrm{d}r^2}\frac{1}{\mathrm{d}\rho/\mathrm{d}r}\Big]\delta\rho\,,\end{aligned} \tag{20}$$

$$P_t(\rho + \delta\rho) = P_t(\rho) + \frac{\mathrm{d}P_t}{\mathrm{d}\rho}\delta\rho\,, \tag{21}$$

$$M(\rho + \delta\rho) = M(\rho) + \frac{\mathrm{d}M}{\mathrm{d}\rho}\delta\rho\,, \tag{22}$$

$$E(\rho + \delta\rho) = E(\rho) + \frac{E'}{\rho'}\delta\rho\,, \tag{23}$$

$$E'(\rho + \delta\rho) = E'(\rho) + \frac{E''}{\rho'}\delta\rho\,. \tag{24}$$

The radial sound speed v_r^2 and tangential sound speed v_t^2 are defined as

$$v_r^2 = \frac{\mathrm{d}P_r}{\mathrm{d}\rho}, \quad v_t^2 = \frac{\mathrm{d}P_t}{\mathrm{d}\rho}\,. \tag{25}$$

The perturbed form of Eq. (18) is given by

$$\Omega = \Omega_0(\rho, P_r,\ P_r',\ P_t,\ M, E, E') + \delta\Omega\,, \tag{26}$$

where

$$\begin{aligned}\delta\Omega = &\frac{\partial\Omega}{\partial\rho}\delta\rho + \frac{\partial\Omega}{\partial P_r}\delta P_r + \frac{\partial\Omega}{\partial P_r'}\delta P_r' + \frac{\partial\Omega}{\partial P_t}\delta P_t + \frac{\partial\Omega}{\partial M}\delta M \\ &+ \frac{\partial\Omega}{\partial E}\delta E + \frac{\partial\Omega}{\partial E'}\delta E'\,,\end{aligned} \tag{27}$$

which can also be written as

$$\begin{aligned}\frac{\delta\Omega}{\delta\rho} = &\frac{\partial\Omega}{\partial\rho} + \frac{\partial\Omega}{\partial P_r}v_r^2 + \frac{\partial\Omega}{\partial P_r'}(v_r^{2\prime} + v_r^2\rho''(\rho')^{-1}) + \frac{\partial\Omega}{\partial P_t}v_t^{2\prime} \\ &+ \frac{4\pi r^2}{\rho'}\frac{\partial\Omega}{\partial M}\Big(\rho + \frac{E^2}{2}\Big) + \frac{\partial\Omega}{\partial E}\frac{E'}{\rho\prime} + \frac{\partial\Omega}{\partial E'}\frac{E''}{\rho'}\,.\end{aligned} \tag{28}$$

This is the fundamental equation used to determine the effect of local DP on the cracking of charged anisotropic fluid. We will plot $\delta\Omega/\delta\rho$ against radius "r" of the star for different values of the parameters involved in the model. Using Eq. (18), the derivatives involved in the above equation are given by

$$\frac{\partial\Omega}{\partial\rho} = \frac{-4M - 16\pi r^3P_r + 3r^3E^2}{4r^2 - 8Mr + 4r^4E^2}\,, \tag{29}$$

$$\frac{\partial\Omega}{\partial M} = -\frac{(\rho + P_r)(4r^2 - 16\pi r^4P_r - 2r^4E^2)}{(2r^2 - 4Mr + 2r^4E^2)^2}\,, \tag{30}$$

$$\begin{aligned}\frac{\partial\Omega}{\partial P_r} = &-\frac{2}{r} - \frac{2M + 16\pi r^3P_r + 8\pi r^3\rho - r^3E^2}{2r^2 - 4Mr + 2r^4E^2} \\ &+ \frac{r^2E^2}{4r - 8M + 4r^3E^2}\,,\end{aligned} \tag{31}$$

$$\frac{\partial\Omega}{\partial P_t} = \frac{2}{r}, \quad \frac{\partial\Omega}{\partial P_r'} = -1\,, \tag{32}$$

$$\begin{aligned}\frac{\partial\Omega}{\partial E} = &-\frac{(\rho + P_r)(r^2E)(3r - 10M + 6r^3E^2 - 6\pi r^3P_r)}{2(r - 2M + r^3E^3)^2} \\ &+ \frac{2 + rE'}{8\pi r}\,,\end{aligned} \tag{33}$$

$$\frac{\partial\Omega}{\partial E'} = \frac{E}{8\pi}\,. \tag{34}$$

4 Cracking of Quark Star Models

In this section, we apply the general formalism developed in the above section for cracking of charged QS to the model given by Maharaj.[26] The model selected here can be applied to QS for different inner matter configurations; isotropic, charged isotropic, anisotropic and charged anisotropic fluid for suitable values of parameters involve in the model of QS. The model selected here is consistent with previously developed charged QS models[5−6] and uncharged QS models[4,8] by taking $A_0 = 0$. The model is defined by means of mass M, density ρ, anisotropy Δ, radial pressure P_r, tangential pressure P_t and electromagnetic field E are given in appendix (see Eqs. (A1)–(A9)).

Also, the radial and tangential sound speed velocities can be obtained from Eqs. (A3) and (A4) and are given in appendix (see Eqs. (A10) and (A11)).

The constants a, B, C, A_1, A_2 and A_3 have dimension of length (L^{-2}). The model presented here is more general and have flexibility of letting various choices of parameters. The suitable choice of parameters allows us to regain stellar masses and radii of compact objects as identified by many research groups. These parameters are given by the following relations; $\tilde{a} = a\Re^2$, $\tilde{B} = B\Re^2$, $\tilde{C} = C\Re^2$, $\tilde{A}_1 = A_1\Re^2$, $\tilde{A}_2 = A_2\Re^2$, $\tilde{A}_3 = A_3\Re^2$, where $\Re$ has the same units as r and in order to match with realistic units, it is given by $\Re = 43.245$ km. Table 1 shows both charged and uncharged QS model corresponding to different choices of parameters.[27] Tables 2 and 3 depict cracking points of QS represented by R_1, R_2, R_3 and R_s corresponding to charged anisotropic, anisotropic, charged isotropic, and isotropic fluid respectively.

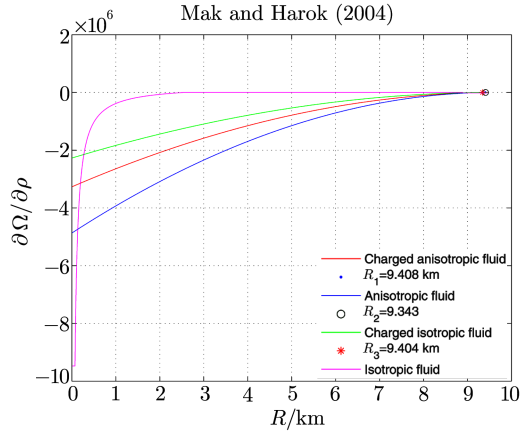

Fig. 1 (Color online) Plots show that cracking takes place for charged anisotropic (red curve), anisotropic (blue curve) and charged isotropic (green curve) fluids with cracking points R_1, R_2 and R_3 respectively. The purple curve shows that the model remains stable (no cracking) for isotropic fluid distribution.

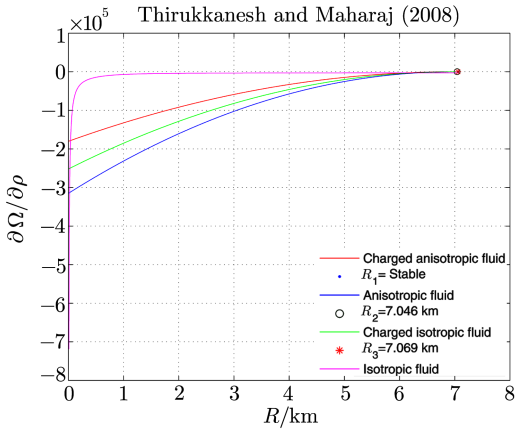

Fig. 2 (Color online) Stability regions of Thirukkanesh and Maharaj model corresponding to charged anisotropic (red curve), anisotropic (blue curve), charged isotropic (green curve) and isotropic (purple curve) fluids.

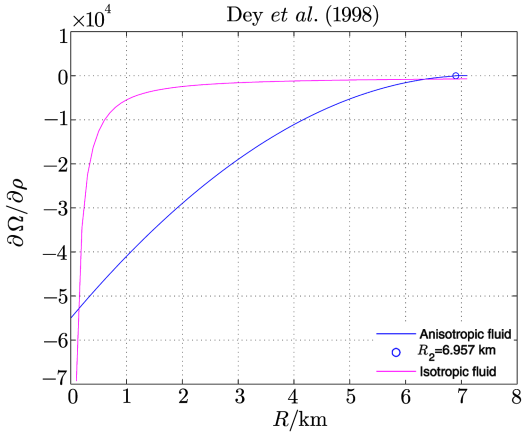

Fig. 3 (Color online) Stability regions of uncharged quark star for isotropic and anisotropic fluids.

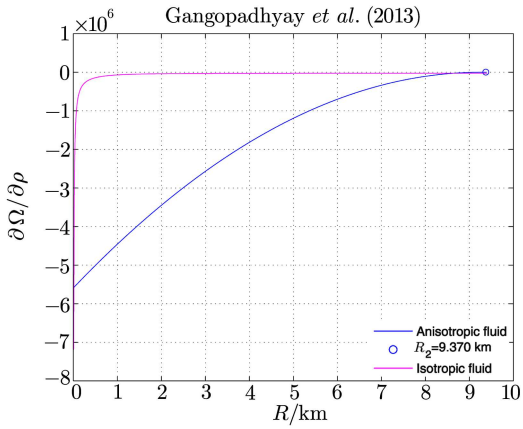

Fig. 4 (Color online) Stability regions of uncharged quark star for isotropic and anisotropic fluids.

For the sake of stability regions of QS, we have plotted force distribution against radius for different values of the parameters involved in the model shown in Figures 1–4. We summarize these results as follows

- Figure 1 represents the stability regions of charged QS obtained by Mak and Harko.[5] We see that cracking take place for charged isotopic, anisotropic and charged anisotropic fluids with cracking points $R_3 = 9.404$ km, $R_2 = 9.343$ km and $R_1 = 9.408$ km (given in Table 2), respectively. These cracking points are labeled by the symbols "$*$", "o" and "." for charged anisotropic, anisotropic, and charged isotropic fluids respectively. However, the system remains stable (no cracking) for isotropic fluid distribution and represented by R_s in Tables 2, 3.
- Figure 2 deals with investigation of cracking

of charged QS presented by Thirukkanesh and Maharaj.[6] We note that cracking takes place for charged isotropic and anisotropic fluids. The cracking points are labeled by $R_2 = 7.046$ km and $R_3 = 7.069$ km for anisotropic and charged isotropic fluids, respectively and are represented by the symbols "o" and "$*$" as shown in the figures. It is worth mentioning here that unlike in the above case, the given model remains stable for the charged anisotropic fluid.

- Figures 3 and 4 show that blue curve changes its sign from negative to positive for anisotropic fluid both for uncharged QS models presented by Dey *et al.*[4] and Gangopadhyay *et al.*,[8] while purple curve does not change its sign. We conclude that the given model is stable for isotropic fluid distribution but exhibits cracking for anisotropic fluid represented by symbol "o" with cracking point R_2 given in Table 3.

Table 1 Various parameter values for various models of QS.[27]

Model	$\tilde{a}$	$\tilde{B}$	$\tilde{C}$	$\tilde{A}_1$	$\tilde{A}_2$	$\tilde{A}_3$	Radius/km	Mass
Dey[4]	202	12	1	25	20	20	7.07	$1.433M_{\odot}$
Mak[5]	52	12	1	20	25	20	9.46	$2.86M_{\odot}$
Thirukkanesh[6]	350	12	1	289	200	260	7.07	$0.94M_{\odot}$
Gangopadhyay[8]	350	12	1	230	235	240	9.40	$1.67M_{\odot}$

Table 2 Cracking of charged quark star models.

Model	R_1/km	R_2/km	R_3/km	R_s/km
Mak and Harok[5]	9.408	9.343	9.404	Stable
Thirukkanesh and Maharaj[6]	Stable	7.046	7.069	Stable

Table 3 Cracking of uncharged quark star models.

Model	R_2/km	R_s/km
Dey *et al.*[4]	6.957	Stable
Gangopadhyay *et al.*[8]	9.370	Stable

5 Outlook

We have applied the technique of cracking presented by Herrera[9] to QS. The idea of cracking helps us to understand the behavior of inner fluid distribution just after departure from equilibrium state. The DP may be responsible for cracking (overturning) of anisotropic sphere.[9] In his study, the global DP affects physical quantities like mass, tangential and radial pressure but does not effect pressure gradient. In this work, we have used local DP technique instead of global DP[17−18] to study cracking of QS with electromagnetic field.

The impact of local DP on the stability of inner fluid of QS with and without charge is considered with isotropic and anisotropic configurations in the framework of GR. It has been observed that cracking of QS takes place when the system leaves its equilibrium state. The numerical value of R_i, $i = 1, 2, 3$ (cracking points) provides the stable region in the QS with SS EoS.

We have used the model of Maharaj *et al.*[26] to investigate the cracking of charged and uncharged QS. Figures 1, 2 correspond to the stability of QS in the presence of charge for different values of parameters given in Table 1. It is shown that QS remains stable, when isotropic inner matter configuration with SS EoS is considered in neutral case but it may exhibit cracking with the inclusion of charge and anisotropy. In Figs. 3, 4, we have given the comparison of stability region of QS[4,8] in neutral case. In these figures stability regions are plotted for isotropic and anisotropic inner matter configurations. These QS are stable for isotropic fluid but exhibit cracking when inner fluid configuration is changed to anisotropic fluid. The observe values of R_i, $i = 1, 2, 3$ are given in Tables 2, 3 for different values of parameters presented in Table 1.

It is noted that the local DP scheme does not affect the stability of QS (remains stable) in neutral case with isotropic inner matter configuration, while changes its stability (potentially unstable) drastically with the inclusion of charge. Such phenomenon is also observed when inner matter configuration is changed from isotropic to anisotropic fluid. Thus the local DP technique under SS linear EoS considerably effects the stability regions of QS. When physical parameters like mass, electromagnetic field and density of QS are locally perturbed they drastically effect the sensitivity of radial forces which may lead towards the gravitational collapse. We conclude that the binding forces of QS may become weaker as we move away from the center of QS and it becomes less dense as charge introduced or inner matter type is changed from isotropic to anisotropic fluid. Finally, we conclude that the QS may exhibit cracking in the presence of electromagnetic field and anisotropic fluid.

Appendix: Definition of the Quantities in the Selected Model

The quantities are defined as follows

$$
\begin{aligned}
M(r) = {} & \frac{\sqrt{3a}\arctan(\sqrt{\frac{3r}{a}})}{3C^{3/2}}\Big(\frac{157A_3a^4}{57\ 915} - \frac{100A_2a^3}{9009} + \frac{59A_1a^2}{1155} + \frac{188Ba}{315} + \frac{129C}{35}\Big) \\
& - \Big(\frac{r}{C}\Big)^{3/2}\Big(\frac{14A_3a^3}{1287} - \frac{10A_2a^2}{429} + \frac{2A_1a}{33} + \frac{B}{9}\Big) - \arctan\Big(\sqrt{\frac{r}{a}}\Big) \\
& \times \sqrt{\frac{a}{C^3}}\Big(\frac{31A_3a^4}{2145} - \frac{31A_2a^3}{100} + \frac{31A_1a^2}{385} + \frac{62Ba}{105} + \frac{93C}{35}\Big) \\
& - \frac{\sqrt{r}(\frac{3A_3a^5}{715} - \frac{9A_2a^4}{1001} + \frac{9A_1a^3}{385} + \frac{6Ba^2}{35} + \frac{27Ca}{35})}{C^{3/2}(a+r)} \\
& - \frac{\sqrt{r}\Big(\frac{8\ 334\ 452\ 270\ 777\ 287A_3a^5}{9\ 223\ 372\ 036\ 854\ 775\ 808} - \frac{100A_2a^4}{27\ 027} + \frac{59A_2a^3}{3465} + \frac{188Ba^2}{945} + \frac{43Ca}{35}\Big)}{C^{3/2}(a+3r)} \\
& - \frac{\sqrt{r}(\frac{2A_3a^6}{2145} - \frac{2A_2a^5}{1001} + \frac{2A_1a^4}{385} + \frac{4Ba^3}{105} + \frac{6Ca^2}{35})}{C^{3/2}(a+r)^2} \\
& - A_3\Big(\frac{r^2}{30} + \frac{14ar}{585} - \frac{1268a}{96\ 525}\Big) - \frac{r^{5/2}(\frac{74A_2}{2145} - \frac{7A_1}{110} + \frac{4r}{91})}{C^{3/2}}\,, \qquad \text{(A1)}
\end{aligned}
$$

$$
\begin{aligned}
\rho = {} & \frac{B(210a^5 + 798a^4r + 1476a^3r^2 + 2540a^2r^3 + 2090ar^4 + 630r^5)}{105(a+r)^3(a+3r)^2} \\
& + \frac{3C(140a^4 + 434a^3r + 318a^2r^2 + 150ar^3 + 30r^4)}{35(a+r)^3(a+3r)^2} + \frac{3\psi(r)}{105(a+r)^3(a+3r)^2}\,, \qquad \text{(A2)}
\end{aligned}
$$

$$
\begin{aligned}
P_r = {} & -\frac{B(70a^5 + 994a^4r + 3708a^3r^2 + \frac{16\ 780a^2r^3}{3} + \frac{11\ 770ar^4}{3} + 1050r^5)}{105(a+r)^3(a+3r)^2} \\
& + \frac{C(140a^4 + 434a^3r + 318a^2r^2 + 150ar^3 + 30r^4)}{35(a+r)^3(a+3r)^2} + \frac{\psi(r)}{105(a+r)^3(a+3r)^2}\,, \qquad \text{(A3)}
\end{aligned}
$$

$$
\begin{aligned}
P_t = {} & -\frac{B(70a^5 + 994a^4r + 3708a^3r^2 + \frac{16\ 780a^2r^3}{3} + \frac{11\ 770ar^4}{3} + 1050r^5)}{105(a+r)^3(a+3r)^2} \\
& + \frac{C(140a^4 + 434a^3r + 318a^2r^2 + 150ar^3 + 30r^4)}{35(a+r)^3(a+3r)^2} + \frac{\psi_1(r)}{105(a+r)^3(a+3r)^2}\,, \qquad \text{(A4)}
\end{aligned}
$$

$$
\Delta = A_3r^3 + A_2r^2 + A_1r\,, \qquad \text{(A5)}
$$

$$
\begin{aligned}
E^2 = {} & -\frac{\psi_2(r) - C(1764a^3r + 13\ 068a^2r^2 + 12\ 204ar^3 + 3780r^4)}{315(a+r)^3(a+3r)^2} \\
& - \frac{B(168a^4r + 1296a^3r^2 + 6528a^2r^3 + 7280ar^4 + 2520r^5)}{315(a+r)^3(a+3r)^2}\,, \qquad \text{(A6)}
\end{aligned}
$$

where

$$
\begin{aligned}
\psi(r) = {} & A_1r\Big(-21a^5 - 57a^4r + 20a^3r^2 + \frac{1360a^2r^3}{3} + 105ar^4 + \frac{315r^5}{11}\Big) \\
& - A_2r^2\Big(\frac{45a^5}{2} + \frac{185a^4r}{2} + \frac{1145a^3r^2}{11} + \frac{315a^2r^3}{13} - \frac{7245ar^4}{286} - \frac{315r^5}{26}\Big) \\
& - A_3r^3\Big(\frac{70a^5}{3} + \frac{3710a^4r}{33} + \frac{2310a^3r^2}{13} + \frac{17\ 206a^2r^3}{143} + \frac{392ar^4}{13}\Big)\,, \qquad \text{(A7)}
\end{aligned}
$$

$$
\begin{aligned}
\psi_1(r) = {} & A_2r^2\Big(\frac{165a^5}{2} + \frac{1705a^4r}{2} + \frac{33\ 505a^3r^2}{11} + \frac{62\ 474a^2r^3}{13} + \frac{24\ 885r^5}{26} + \frac{7\ 675\ 321\ 606\ 664\ 163ar^4}{2\ 199\ 023\ 255\ 552}\Big) \\
& + A_3r^3\Big(\frac{3080a^5}{3} + \frac{27\ 475a^4r}{33} + \frac{38\ 640a^3r^2}{13} + \frac{5\ 178\ 346\ 077\ 769\ 871a^2r^3}{1\ 099\ 511\ 627\ 776} + \frac{44\ 653ar^4}{13}\Big) \\
& + A_1r\Big(84a^5 + 888a^4r + 3170a^3r^2 + \frac{54\ 490a^2r^3}{11} + 3570ar^4 + \frac{10\ 710r^5}{11}\Big)\,, \qquad \text{(A8)}
\end{aligned}
$$

$$\begin{aligned}\psi_2(r) = {} & A_2 r^2\Big(225a^5 + 1845a^4 r + \frac{63\ 210a^3r^2}{11} + \frac{8\ 714\ 360\ 094\ 912\ 483a^2r^3}{1\ 099\ 511\ 627\ 776} + \frac{55\ 755ar^4}{11} + \frac{16\ 065r^5}{13}\Big) \\ & + A_3 r^3\Big(1344a^5 + \frac{18\ 550a^4 r}{11} + \frac{2\ 838\ 585\ 333\ 862\ 543a^3r^2}{549\ 755\ 813\ 888} + \frac{78\ 624a^2r^3}{11} + \frac{59\ 934ar^4}{13}\Big) \\ & + A_1 r\Big(252a^5 + 2124a^4 r + 6732a^3r^2 + \frac{5\ 016\ 771\ 690\ 734\ 313a^2r^3}{549\ 755\ 813\ 888} + \frac{63\ 000ar^4}{11} + \frac{15\ 120r^5}{11}\Big),\end{aligned} \tag{A9}$$

$$\begin{aligned}v_r^2 = {} & -\Bigg[\Big\{B\Big(70a^5 + 994a^4 r + 3708a^3r^2 + \frac{16\ 780a^2r^3}{3} + \frac{11\ 770ar^4}{3} + 1050r^5\Big) \\ & + A_2 r^2\Big(\frac{45a^5}{2} + \frac{185a^4 r}{2} + \frac{1145a^3r^2}{11} + \frac{315a^2r^3}{13} - \frac{7245ar^4}{286} - \frac{315r^5}{26}\Big) \\ & - A_1 r\Big(-21a^5 - 57a^4 r + 20a^3r^2 + \frac{1360a^2r^3}{3} + 105ar^4 + \frac{315r^5}{11}\Big) \\ & + A_3 r^3\Big(\frac{70a^5}{3} + \frac{3710a^4 r}{33} + \frac{2310a^3r^2}{13} + \frac{17\ 206a^2r^3}{143} + \frac{392ar^4}{13}\Big)\Big\}(35(a+r)^4(a+3r)^2)^{-1} \\ & + \Big\{2B\Big(70a^5 + 994a^4 r + 3708a^3r^2 + \frac{16\ 780a^2r^3}{3} + \frac{11\ 770ar^4}{3} + 1050r^5\Big) \\ & + 2A_2 r^2\Big(\frac{45a^5}{2} + \frac{185a^4 r}{2} + \frac{1145a^3r^2}{11} + \frac{315a^2r^3}{13} - \frac{7245ar^4}{286} - \frac{315r^5}{26}\Big) \\ & - 2A_1 r\Big(-21a^5 - 57a^4 r + 20a^3r^2 + \frac{1360a^2r^3}{3} + 105ar^4 + \frac{315r^5}{11}\Big) \\ & + 2A_3 r^3\Big(\frac{70a^5}{3} + \frac{3710a^4 r}{33} + \frac{2310a^3r^2}{13} + \frac{17\ 206a^2r^3}{143} + \frac{392ar^4}{13}\Big)\Big\}(35(a+r)^3(a+3r)^3)^{-1} \\ & - \Big\{B\Big(994a^4 + 7416a^3 r + 16\ 780a^2r^2 + \frac{47\ 080ar^3}{3} + 5250r^4\Big) \\ & - A_1\Big(-21a^5 - 57a^4 r + 20a^3r^2 + \frac{1360a^2r^3}{3} + 105ar^4 + \frac{315r^5}{11}\Big) \\ & + A_3 r^3\Big(\frac{3710a^4}{33} + \frac{4620a^3 r}{13} + \frac{51\ 618a^2r^2}{143} + \frac{1568ar^3}{13}\Big) \\ & + A_2 r^2\Big(\frac{185a^4}{2} + \frac{2290a^3 r}{11} + \frac{945a^2r^2}{13} - \frac{14\ 490ar^3}{143} - \frac{1575r^4}{26}\Big) \\ & + 2A_2 r\Big(\frac{45a^5}{2} + \frac{185a^4 r}{2} + \frac{1145a^3r^2}{11} + \frac{315a^2r^3}{13} - \frac{7245ar^4}{286} - \frac{315r^5}{26}\Big) \\ & - A_1 r\Big(-57a^4 + 40a^3 r + 1360a^2r^2 + 420ar^3 + \frac{1575r^4}{11}\Big) \\ & + 3A_3 r^2\Big(\frac{70a^5}{3} + \frac{3710a^4 r}{33} + \frac{2310a^3r^2}{13} + \frac{17\ 206a^2r^3}{143} + \frac{392ar^4}{13}\Big)\Big\}(105(a+r)^3(a+3r)^2)^{-1} \\ & - \frac{6C(140a^4 + 434a^3 r + 318a^2r^2 + 150ar^3 + 30r^4)}{35(a+r)^3(a+3r)^3} \\ & - \frac{3C(140a^4 + 434a^3 r + 318a^2r^2 + 150ar^3 + 30r^4)}{35(a+r)^4(a+3r)^2} + \frac{C(434a^3 + 636a^2 r + 450ar^2 + 120r^3)}{35(a+r)^3(a+3r)^2}\Bigg] \\ & \Big/\Bigg[\Big\{\Big\{B(210a^5 + 798a^4 r + 1476a^3r^2 + 2540a^2r^3 + 2090ar^4 + 630r^5) \\ & - 3A_2 r^2\Big(\frac{45a^5}{2} + \frac{185a^4 r}{2} + \frac{1145a^3r^2}{11} + \frac{315a^2r^3}{13} - \frac{7245ar^4}{286} - \frac{315r^5}{26}\Big) \\ & + 3A_1 r\Big(-21a^5 - 57a^4 r + 20a^3r^2 + \frac{1360a^2r^3}{3} + 105ar^4 + \frac{315r^5}{11}\Big) \\ & - 3A_3 r^3\Big(\frac{70a^5}{3} + \frac{3710a^4 r}{33} + \frac{2310a^3r^2}{13} + \frac{17\ 206a^2r^3}{143} + \frac{392ar^4}{13}\Big)\Big\}(35(a+r)^4(a+3r)^2)^{-1} \\ & + \Big\{2B(210a^5 + 798a^4 r + 1476a^3r^2 + 2540a^2r^3 + 2090ar^4 + 630r^5)\end{aligned}$$

$$
\begin{aligned}
&- 6A_2r^2\Big(\frac{45a^5}{2}+\frac{185a^4r}{2}+\frac{1145a^3r^2}{11}+\frac{315a^2r^3}{13}-\frac{7245ar^4}{286}-\frac{315r^5}{26}\Big)\\
&+ 6A_1r\Big(-21a^5-57a^4r+20a^3r^2+\frac{1360a^2r^3}{3}+105ar^4+\frac{315r^5}{11}\Big)\\
&- 6A_3r^3\Big(\frac{70a^5}{3}+\frac{3710a^4r}{33}+\frac{2310a^3r^2}{13}+\frac{17\ 206a^2r^3}{143}+\frac{392ar^4}{13}\Big)\Big\}(35(a+r)^3(a+3r)^3)^{-1}\\
&+\Big\{3A_3r^3\Big(\frac{3710a^4}{33}+\frac{4620a^3r}{13}+\frac{51\ 618a^2r^2}{143}+\frac{1568ar^3}{13}\Big)\\
&- B(798a^4+2952a^3r+7620a^2r^2+8360ar^3+3150r^4)\\
&- 3A_1\Big(-21a^5-57a^4r+20a^3r^2+\frac{1360a^2r^3}{3}+105ar^4+\frac{315r^5}{11}\Big)\\
&+ 3A_2r^2\Big(\frac{185a^4}{2}+\frac{2290a^3r}{11}+\frac{945a^2r^2}{13}-\frac{14\ 490ar^3}{143}-\frac{1575r^4}{26}\Big)\\
&+ 6A_2r\Big(\frac{45a^5}{2}+\frac{185a^4r}{2}+\frac{1145a^3r^2}{11}+\frac{315a^2r^3}{13}-\frac{7245ar^4}{286}-\frac{315r^5}{26}\Big)\\
&- 3A_1r\Big(-57a^4+40a^3r+1360a^2r^2+420ar^3+\frac{1575r^4}{11}\Big)\\
&+ 9A_3r^2\Big(\frac{70a^5}{3}+\frac{3710a^4r}{33}+\frac{2310a^3r^2}{13}+\frac{17\ 206a^2r^3}{143}+\frac{392ar^4}{13}\Big)\Big\}(105(a+r)^3(a+3r)^2)^{-1}\\
&+\frac{18C(140a^4+434a^3r+318a^2r^2+150ar^3+30r^4)}{35(a+r)^3(a+3r)^3}\\
&+\frac{9C(140a^4+434a^3r+318a^2r^2+150ar^3+30r^4)}{35(a+r)^4(a+3r)^2}\\
&-\frac{3C(434a^3+636a^2r+450ar^2+120r^3)}{35(a+r)^3(a+3r)^2}\Big\}\Big],
\end{aligned}
\tag{A10}
$$

$$
\begin{aligned}
v_t^2=\Big[&\Big\{A_2r^2\Big(\frac{165a^5}{2}+\frac{1705a^4r}{2}+\frac{33\ 505a^3r^2}{11}+\frac{62\ 474a^2r^3}{13}+\frac{24\ 885r^5}{26}\\
&+\frac{7\ 675\ 321\ 606\ 664\ 163ar^4}{2\ 199\ 023\ 255\ 552}\Big)-B\Big(70a^5+994a^4r+3708a^3r^2+\frac{16\ 780a^2r^3}{3}\\
&+\frac{11\ 770ar^4}{3}+1050r^5\Big)+A_3r^3\Big(\frac{3080a^5}{3}+\frac{27\ 475a^4r}{33}+\frac{38\ 640a^3r^2}{13}\\
&+\frac{5\ 178\ 346\ 077\ 769\ 871a^2r^3}{1\ 099\ 511\ 627\ 776}+\frac{44\ 653ar^4}{13}\Big)+A_1r\Big(84a^5+888a^4r+3170a^3r^2\\
&+\frac{54\ 490a^2r^3}{11}+3570ar^4+\frac{10\ 710r^5}{11}\Big)\Big\}(35(a+r)^4(a+3r)^2)^{-1}\\
&+\Big\{2A_2r^2\Big(\frac{165a^5}{2}+\frac{1705a^4r}{2}+\frac{33\ 505a^3r^2}{11}\\
&+\frac{62\ 474a^2r^3}{13}+\frac{767\ 532\ 1606\ 664\ 163ar^4}{2\ 199\ 023\ 255\ 552}+\frac{24\ 885r^5}{26}\Big)-2B\Big(70a^5+994a^4r\\
&+3708a^3r^2+\frac{16\ 780a^2r^3}{3}+\frac{11\ 770ar^4}{3}+1050r^5\Big)+2A_3r^3\Big(\frac{3080a^5}{3}\\
&+\frac{27\ 475a^4r}{33}+\frac{38\ 640a^3r^2}{13}+\frac{5\ 178\ 346\ 077\ 769\ 871a^2r^3}{1\ 099\ 511\ 627\ 776}+\frac{44\ 653ar^4}{13}\Big)\\
&+2A_1r\Big(84a^5+888a^4r+3170a^3r^2+\frac{54\ 490a^2r^3}{11}+3570ar^4+\frac{10\ 710r^5}{11}\Big)\Big\}(35(a+r)^3(a+3r)^3)^{-1}\\
&-\Big\{A_1\Big(84a^5+888a^4r+3170a^3r^2+\frac{54\ 490a^2r^3}{11}+3570ar^4+\frac{10\ 710r^5}{11}\Big)\\
&-B\Big(994a^4+7416a^3r+16\ 780a^2r^2+\frac{47\ 080ar^3}{3}+5250r^4\Big)\\
&+A_3r^3\Big(\frac{27\ 475a^4}{33}+\frac{77\ 280a^3r}{13}+\frac{3\ 883\ 759\ 558\ 327\ 403a^2r^2}{274\ 877\ 906\ 944}+\frac{178\ 612ar^3}{13}\Big)
\end{aligned}
$$

$$
\begin{aligned}
&+A_2r^2\Big(\frac{1705a^4}{2}+\frac{67\ 010a^3r}{11}+\frac{187\ 422a^2r^2}{13}+\frac{7\ 675\ 321\ 606\ 664\ 163ar^3}{549\ 755\ 813\ 888}+\frac{124\ 425r^4}{26}\Big)\\
&+3A_3r^2\Big(\frac{3080a^5}{3}+\frac{27475a^4r}{33}+\frac{38\ 640a^3r^2}{13}+\frac{5178346\ 077\ 769\ 871a^2r^3}{1\ 099\ 511\ 627\ 776}+\frac{44\ 653ar^4}{13}\Big)\\
&+A_1r\Big(888a^4+6340a^3r+\frac{163\ 470a^2r^2}{11}+14\ 280ar^3+\frac{53\ 550r^4}{11}\Big)\\
&+2A_2r\Big(\frac{165a^5}{2}+\frac{1705a^4r}{2}+\frac{33\ 505a^3r^2}{11}+\frac{62\ 474a^2r^3}{13}\\
&+\frac{7\ 675\ 321\ 606\ 664\ 163ar^4}{2\ 199\ 023\ 255\ 552}+\frac{24\ 885r^5}{26}\Big)\Big\}(105(a+r)^3(a+3r)^2)^{-1}\\
&+\frac{6C(140a^4+434a^3r+318a^2r^2+150ar^3+30r^4)}{35(a+r)^3(a+3r)^3}\\
&+\frac{3C(140a^4+434a^3r+318a^2r^2+150ar^3+30r^4)}{35(a+r)^4(a+3r)^2}-\frac{C(434a^3+636a^2r+450ar^2+120r^3)}{35(a+r)^3(a+3r)^2}\Bigg]\\
&\Bigg/\Bigg[\Big\{B(210a^5+798a^4r+1476a^3r^2+2540a^2r^3+2090ar^4+630r^5)\\
&-3A_2r^2\Big(\frac{45a^5}{2}+\frac{185a^4r}{2}+\frac{1145a^3r^2}{11}+\frac{315a^2r^3}{13}-\frac{7245ar^4}{286}-\frac{315r^5}{26}\Big)\\
&+3A_1r\Big(-21a^5-57a^4r+20a^3r^2+\frac{1360a^2r^3}{3}+105ar^4+\frac{315r^5}{11}\Big)\\
&-3A_3r^3\Big(\frac{70a^5}{3}+\frac{3710a^4r}{33}+\frac{2310a^3r^2}{13}+\frac{17\ 206a^2r^3}{143}+\frac{392ar^4}{13}\Big)\Big\}(35(a+r)^4(a+3r)^2)^{-1}\\
&+\Big\{2B(210a^5+798a^4r+1476a^3r^2+2540a^2r^3+2090ar^4+630r^5)\\
&-6A_2r^2\Big(\frac{45a^5}{2}+\frac{185a^4r}{2}+\frac{1145a^3r^2}{11}+\frac{315a^2r^3}{13}-\frac{7245ar^4}{286}-\frac{315r^5}{26}\Big)\\
&+6A_1r\Big(-21a^5-57a^4r+20a^3r^2+\frac{1360a^2r^3}{3}+105ar^4+\frac{315r^5}{11}\Big)\\
&-6A_3r^3\Big(\frac{70a^5}{3}+\frac{3710a^4r}{33}+\frac{2310a^3r^2}{13}+\frac{17\ 206a^2r^3}{143}+\frac{392ar^4}{13}\Big)\Big\}(35(a+r)^3(a+3r)^3)^{-1}\\
&+\Big\{3A_3r^3\Big(\frac{3710a^4}{33}+\frac{4620a^3r}{13}+\frac{51\ 618a^2r^2}{143}+\frac{1568ar^3}{13}\Big)\\
&-B(798a^4+2952a^3r+7620a^2r^2+8360ar^3+3150r^4\Big)\\
&-3A_1\Big(-21a^5-57a^4r+20a^3r^2+\frac{1360a^2r^3}{3}+105ar^4+\frac{315r^5}{11}\Big)\\
&+3A_2r^2\Big(\frac{185a^4}{2}+\frac{2290a^3r}{11}+\frac{945a^2r^2}{13}-\frac{14\ 490ar^3}{143}-\frac{1575r^4}{26}\Big)\\
&+6A_2r\Big(\frac{45a^5}{2}+\frac{185a^4r}{2}+\frac{1145a^3r^2}{11}+\frac{315a^2r^3}{13}-\frac{7245ar^4}{286}-\frac{315r^5}{26}\Big)\\
&-3A_1r\Big(-57a^4+40a^3r+1360a^2r^2+420ar^3+\frac{1575r^4}{11}\Big)\\
&+9A_3r^2\Big(\frac{70a^5}{3}+\frac{3710a^4r}{33}+\frac{2310a^3r^2}{13}+\frac{17\ 206a^2r^3}{143}+\frac{392ar^4}{13}\Big)\Big\}(105(a+r)^3(a+3r)^2)^{-1}\\
&+\frac{18C(140a^4+434a^3r+318a^2r^2+150ar^3+30r^4)}{35(a+r)^3(a+3r)^3}\\
&+\frac{9C(140a^4+434a^3r+318a^2r^2+150ar^3+30r^4)}{35(a+r)^4(a+3r)^2}\\
&-\frac{3C(434a^3+636a^2r+450ar^2+120r^3)}{35(a+r)^3(a+3r)^2}\Bigg]. \qquad \text{(A11)}
\end{aligned}
$$

References

[1] E. Witten, Phys. Rev. D **30** (1984) 272.

[2] X.D. Li, Z.G. Dai, and Z.R. Wang, Astron. Astrophys. **303** (1995) L1.

[3] I. Bombaci, Phys. Rev. C **55** (1997) 1587.

[4] M. Dey, I. Bombaci, J. Dey, S. Ray, and B.C. Samanta, Phys. Lett. B **438** (1998) 123.

[5] M.K. Mak and T. Harko, Int. J. Mod. Phys. D **13** (2004) 149.

[6] S. Thirukkanesh and S.D. Maharaj, Class. Quantum Grav. **25** (2008) 235001.

[7] R.P. Negreiros, F. Weber, M. Malheiro, and V. Usov, Phys. Rev. D **80** (2009) 083006.

[8] T. Gangopadhyay, S. Ray, X.D. Li, J. Dey, and M. Dey, Mon. Not. R. Astron. Soc. **431** (2013) 3216.

[9] L. Herrera, Phys. Lett. A **165** (1992) 206.

[10] L. Herrera and N.O. Santos, Phys. Rep. **286** (1997) 53.

[11] L. Herrera and V. Varela, Phys. Lett. A **226** (1997) 143.

[12] A. Di Prisco, L. Herrera, and V. Varela, Gen. Rel. Grav. **29** (1997) 1239.

[13] H. Hernandez and L.A. Nunez, Can. J. Phys. **82** (2004) 29.

[14] H. Abreu, H. Hernandez, and L.A. Nunez, J. Phys. Con. Ser. **66** (2006) 012038.

[15] H. Abreu, H. Hernandez, and L.A. Nunez, Class. Quant. Grav. **24** (2007) 4631.

[16] J. Manjarrez, L.A. Nunez, and U. Percoco, Integ. Rev. **25** (2007) 159.

[17] G.A. Gonzalez, A. Navarro, and L.A. Nunez, arXiv:[gr-qc] 1410.7733 (2014).

[18] G.A. Gonzalez, A. Navarro, and L.A. Nunez, J. Phys. Conf. Ser. **600** (2015) 012014.

[19] M. Azam, S.A. Mardan, and M.A. Rehman, Astrophys. Space Sci. **358** (2015) 6.

[20] M. Azam, S.A. Mardan, and M.A. Rehman, Astrophys. Space Sci. **359** (2015) 14.

[21] W.B. Bonnor, Zeit. Phys. **160** (1960) 59.

[22] W.B. Bonnor, Mon. Not. R. Astron. Soc. **129** (1964) 443.

[23] S. Ray and M. Malheiro, Braz. J. Phys. **34** (2004) 310.

[24] M. Sharif and M. Azam, Chin. Phys. B **22** (2013) 050401.

[25] M. Sharif and M. Azam, Eur. Phys. J. C **73** (2013) 2407.

[26] S.D. Maharaj, S. Ray, and M.J. Sunzu, Eur. Phys. J. Plus **129** (2014) 3.

[27] M.J. Sunzu, S.D. Maharaj, and S. Ray, Astrophys. Space Sci. **352** (2015) 719.

[28] K. Johnson, Act. Phys. Pol. B **6** (1975) 865.